Published OnlineFirst February 2, 2010; DOI: 10.1158/1535-7163.MCT-09-0872

Research Article

Molecular Cancer Therapeutics

ATM Deficiency Sensitizes Mantle Cell Lymphoma Cells to Poly(ADP-Ribose) Polymerase-1 Inhibitors

Chris T. Williamson[1,3], Huong Muzik[2,3], Ali G. Turhan[4], Alberto Zamò[5], Mark J. O'Connor[6], D. Gwyn Bebb[2,3], and Susan P. Lees-Miller[1,2,3]

Abstract

Poly(ADP-ribose) polymerase-1 (PARP-1) inhibition is toxic to cells with mutations in the breast and ovarian cancer susceptibility genes *BRCA1* or *BRCA2*, a concept termed synthetic lethality. However, whether this approach is applicable to other human cancers with defects in other DNA repair genes has yet to be determined. The *ataxia telangiectasia mutated* (*ATM*) gene is altered in several human cancers including mantle cell lymphoma (MCL). Here, we characterize a panel of MCL cell lines for ATM status and function and investigate the potential for synthetic lethality in MCL in the presence of small-molecule inhibitors of PARP-1. We show that Granta-519 and UPN2 cells have low levels of ATM protein, are defective in DNA damage-induced ATM-dependent signaling, are radiation sensitive, and have cell cycle checkpoint defects: all characteristics of defective ATM function. Significantly, Granta-519 and UPN2 cells were more sensitive to PARP-1 inhibition than were the ATM-proficient MCL cell lines examined. Furthermore, the PARP-1 inhibitor olaparib (known previously as AZD2281/KU-0059436) significantly decreased tumor growth and increased overall survival in mice bearing s.c. xenografts of ATM-deficient Granta-519 cells while producing only a modest effect on overall survival of mice bearing xenografts of the ATM-proficient cell line, Z138. Thus, PARP inhibitors have therapeutic potential in the treatment of MCL, and the concept of synthetic lethality extends to human cancers with *ATM* alterations. *Mol Cancer Ther; 9(2); 347–57. ©2010 AACR.*

Introduction

Cells are continuously exposed to exogenous agents and biological processes that create DNA damage, which, if not repaired effectively and efficiently, can lead to genomic instability or cell death (1). It follows that cells that are compromised in one DNA repair pathway may be more susceptible to inhibition of a compensatory repair pathway, leading to new opportunities for therapeutic intervention for a variety of human malignancies. The efficacy of this approach, termed synthetic lethality (2–5), has been shown by the use of small-molecule inhibitors of the DNA damage response protein poly(ADP-ribose) polymerase-1 (PARP-1; ref. 6) in cells bearing mutations in the genes encoding DNA double-strand break (DSB) repair proteins, BRCA1 or BRCA2 (7, 8). The synthetic lethal approach may be applicable to cells with alterations in other DNA repair genes (9–13); however, whether synthetic lethality is applicable to other human cancers that have acquired mutations/deletions in DNA repair genes has not been determined.

Here, we test the synthetic lethality approach for an important human malignancy, mantle cell lymphoma (MCL), to determine whether alterations to *ataxia telangiectasia mutated* (*ATM*) that arise during oncogenic transformation sensitize cells to PARP-1 inhibitors. MCL comprises ~10% of all non-Hodgkin's lymphoma and has the lowest median survival of any non-Hodgkin's lymphoma at 3 years post-diagnosis (14). The genetic hallmark of MCL is a chromosomal translocation t(11;14)(q13;q32) that juxtaposes *IgH* gene promoter elements upstream of *CCND1* (15). This translocation leads to overexpression of cyclin D1, which promotes progression through the G_1-S cell cycle checkpoint (16, 17). Importantly, 20% to 50% of MCL cases contain mutations in *ATM* (18), and MCL has the highest rate of *ATM* mutation of any non-Hodgkin's lymphoma subtype (19).

ATM is a serine/threonine protein kinase that plays a critical role in DNA damage–induced signaling and the initiation of cell cycle checkpoint signaling in response to DNA-damaging agents such as ionizing radiation (IR; refs. 20, 21). Although ablation of ATM through RNA interference (9), genetic means (12, 13, 22), or inhibition of ATM kinase activity using a small-molecule

Authors' Affiliations: Departments of [1]Biochemistry and Molecular Biology and [2]Oncology and [3]Southern Alberta Cancer Research Institute, University of Calgary, Calgary, Alberta, Canada; [4]Inserm U935, University of Poitiers and Service d'Hématologie et d'Oncologie Biologique EA 3805, CHU de Poitiers, Poitiers, France; [5]Dipartimento di Patologia, Sezione di Anatomia Patologica, University of Verona, Verona, Italy; and [6]KuDOS Pharmaceuticals, Cambridge, United Kingdom

Note: Supplementary material for this article is available at Molecular Cancer Therapeutics Online (http://mct.aacrjournals.org/).

Corresponding Authors: Susan P. Lees-Miller, Department of Biochemistry and Molecular Biology, University of Calgary, 3330 Hospital Drive Northwest, Calgary, Alberta, Canada T2N 4N1. Phone: 403-220-7628; Fax: 403-283-8727. E-mail: leesmill@ucalgary.ca or D. Gwyn Bebb, Department of Oncology, University of Calgary, Tom Baker Cancer Center, 1331 29 Street Northwest, Calgary, Alberta, Canada T2N 4N2. Phone: 403-521-3166; Fax: 403-283-1651. E-mail: Gwyn-Bebb@albertahealthservices.ca

doi: 10.1158/1535-7163.MCT-09-0872

Published OnlineFirst February 2, 2010; DOI: 10.1158/1535-7163.MCT-09-0872

inhibitor sensitizes cells to PARP-1 inhibitors (9), the importance of this approach for human cancers with alterations in *ATM* remains unknown.

Here, we characterized ATM protein function in a panel of patient-derived MCL cell lines: Granta-519, HBL-2, JVM-2, MAVER-1, UPN1, UPN2, and Z138. Both alleles of *ATM* are reported to be wild-type in JVM-2 (23). Granta-519 and UPN2 both contain a single copy of the *ATM* gene that harbors a point mutation in conserved residues within the kinase domain (24, 25). UPN1 cells contain one copy of wild-type *ATM*, with the second allele containing a polymorphism in the NH_2-terminal HEAT repeat region (25). One copy of *ATM* is deleted in MAVER-1, and no sequence information is available regarding the second allele (26). *ATM* status in HBL-2 and Z138 cells has not been reported. All of the MCL cell lines used in this study contain the distinguishing t(11;14)(q13;q32) translocation resulting in *CCND1* (cyclin D1) overexpression (27). p53 and EBV status in the cell lines studied is summarized in Supplementary Table S1. Other genomic alterations in MCL have been described in detail elsewhere (28). Here, we show that Granta-519 and UPN2 cells are defective in ATM function and are sensitive to the PARP-1 inhibitors PJ34 (29) and olaparib (known previously as AZD2281/KU-0059436; ref. 30). Our results suggest that olaparib induces cell death, at least in part, through the induction of apoptosis. Moreover, using a mouse xenograft model of MCL (31), we show that olaparib inhibits tumor growth and increases survival in mice bearing xenografts of the ATM-deficient cell line, Granta-519, and, to a lesser extent, in mice bearing xenografts of the ATM-proficient cell line, Z138. Thus, PARP-1 inhibitors have therapeutic potential in the treatment of ATM-deficient MCL, and our results extend the concept of synthetic lethality to tumors bearing alterations in *ATM*.

Materials and Methods

Cell Lines

Granta-519, HBL-2, JVM-2, MAVER-1, Z138, C35ABR (BT), and L3 cells were cultured in suspension in RPMI 1640 (Invitrogen) containing 10% (v/v) fetal bovine serum (Hyclone), 50 units/mL penicillin, and 50 μg/mL streptomycin at 37°C under 5% CO_2. UPN1 and UPN2 cells were cultured in suspension in MEM-α (Invitrogen) containing 10% fetal bovine serum and antibiotics as above. C35ABR (BT; ATM-proficient) and L3 (ATM-deficient) cell lines were kindly provided by Dr. M. Lavin (Queensland Institute of Medical Research) and Dr. Y. Shiloh (Tel Aviv University), respectively.

Stable Knockdown of ATM in MCL Cell Lines

pSUPER.retro.puro vectors encoding short hairpin RNA (shRNA) to either green fluorescent protein (GFP) or ATM (32) were kindly provided by Dr. Y. Shiloh. *Eco*RI-linearized plasmid DNA (5 μg) was transfected into Z138 cells using Nucleofector Kit V and electroporation (Amaxa Biosystems) according to the manufacturer's instructions. Cells were subsequently serially diluted and treated with 1 μg/mL puromycin to select cells with stable integration of the plasmid. Following 3 weeks of selection in puromycin, viable cells were assayed for the presence of ATM by immunoblotting. Stable cell lines expressing shRNA to GFP were generated in a similar manner.

Ionizing Radiation

Where indicated, cells were irradiated (in medium plus serum) using a ^{137}Cs source Gammacell 1000 tissue irradiator (MDS Nordion) at a dose rate of 3.53 Gy/min.

Generation of Cell Extracts and Immunoblotting. Cells were harvested by centrifugation (500 × *g* for 5 min), washed twice in cold PBS [137 mmol/L NaCl, 1.47 mmol/L KH_2PO_4, 10 mmol/L Na_2HPO_4, and 2.7 mmol/L KCl (pH 7.4)], resuspended in ice cold NET-N lysis buffer [150 mmol/L NaCl, 0.2 mmol/L EDTA, 50 mmol/L Tris-HCl (pH 7.5), and 1% (v/v) NP-40] containing protein phosphatase and protease inhibitors (1 μmol/L microcystin-LR, 0.2 mmol/L phenylmethylsulfonyl fluoride, 0.1 μg/mL pepstatin, 0.1 μg/mL aprotinin, and 0.1 μg/mL leupeptin), and lysed on ice by sonication (2 × 5 s bursts). Total protein [50 μg; as determined by the Detergent-Compatible Protein Assay (Bio-Rad) using bovine serum albumin as standard] was resolved by SDS-PAGE and transferred to nitrocellulose. Membranes were blocked with 20% (w/v) skim milk powder in T-TBS buffer [20 mmol/L Tris-HCl (pH 7.5), 500 mmol/L NaCl, and 0.1% (v/v) Tween 20] and probed with antibodies to total proteins or phosphorylated proteins as indicated. The ATM-specific rabbit polyclonal antibody 4BA was a kind gift from Dr. M. Lavin. The antibody DPK1 to the catalytic subunit of DNA-dependent protein kinase (DNA-PKcs) has been described previously (33). Antibodies to structural maintenance of chromosomes-1 (SMC-1), KRAB-associated protein (KAP-1), PARP-1, cyclin D1, and actin were purchased from Novus, Abcam, Calbiochem, and Sigma-Aldrich, respectively. Phosphospecific antibodies to P-Ser^{1981} ATM, P-Ser^{957} SMC-1, and P-Ser^{966} SMC-1 were purchased from Epitomics, Novus, and Abcam, respectively. The phosphospecific antiserum to KAP-1 (P-S824) was made in-house and described previously (34).

WST-1 Cytotoxicity Assays

Cells (5×10^4/mL) were seeded in 96-well plates in 100 μL serum-supplemented phenol red–free RPMI 1640 or MEM-α (Invitrogen) and incubated overnight at 37°C under 5% CO_2. The PARP-1 inhibitors PJ34 (Sigma-Aldrich) and olaparib were prepared as stock solutions in water or DMSO, respectively, and stored at −80°C until use. PJ34 and/or olaparib were diluted in phenol red–free medium, and 10 μL of the diluted compound were added to each well. Plates were incubated at 37°C under 5% CO_2 for the indicated times before the addition of WST-1 reagent (Roche). After an additional incubation for 1 h, the absorbance at 450 nm was determined on a microplate reader (Bio-Rad). To determine statistical significance, one-way ANOVA tests were run for replicates of three samples,

Published OnlineFirst February 2, 2010; DOI: 10.1158/1535-7163.MCT-09-0872

with Newman-Keuls' post hoc test analysis. P values < 0.05 were considered statistically significant and are indicated on the figures as an asterisk or a number sign.

Trypan Blue Exclusion Assays

Cells were seeded in 10 mL medium and incubated overnight before treatment with inhibitor or an equal volume of vehicle. Following the indicated incubation time, aliquots were removed and cell density and viability were determined by trypan blue exclusion. Statistical analysis was done as above.

Phospho–histone H3 Cell Cycle Checkpoint Assays

Phospho–histone H3 assays were carried out as described (35). Briefly, cells were either unirradiated or irradiated (2 Gy) and allowed to recover for 1 or 24 h at 37°C under 5% CO_2. Cells were then fixed with 0.9% (w/v) NaCl/95% (v/v) ethanol, resuspended in PBS containing 0.25% (v/v) Triton X-100, incubated on ice for 15 min, and incubated in PBS containing 1% bovine serum albumin and 75 μg/mL phospho–histone H3 antibody (Upstate) for 3 h. Samples were then incubated for 30 min at room temperature with FITC goat anti-rabbit antibody (Jackson ImmunoResearch; diluted 1:30 with PBS containing 1% bovine serum albumin), stained with propidium iodide, and analyzed by flow cytometry using a FACScan flow cytometer (Becton Dickinson) and plotted using Modfit by the University of Calgary Flow Cytometry Facility.

Terminal Deoxynucleotidyl Transferase–Mediated dUTP Nick End Labeling Assays

Cells were exposed to olaparib (2.5 μmol/L) for the indicated times and fixed in 1% paraformaldehyde diluted in PBS for 1 h on ice. Terminal deoxynucleotidyl transferase–mediated dUTP nick end labeling (TUNEL) assays were carried out as per the manufacturer's instructions (Apo-Direct kit; Calbiochem).

Annexin V Assays

Cells were exposed to olaparib (2.5 μmol/L) for the indicated times and resuspended in Annexin V binding buffer [10 mmol/L HEPES (pH 7.5), 140 mmol/L NaCl, and 2.5 mmol/L $CaCl_2$] before incubation with FITC-Annexin V (GeneTex) and 5 μg/mL propidium iodide with RNase for 5 min and then analyzed by flow cytometry as described above.

In vivo Studies

All animal procedures were carried out by a trained animal technician in accordance with established procedures at the Animal Resource Center at the University of Calgary. Female $RAG2^{-/-}$ mice (Taconic) were injected s.c. in the right flank with 5×10^6 cells in a 1:1 emulsion of Matrigel (BD Biosciences) as described previously (31). One group of 30 mice was injected with Granta-519 cells (ATM-deficient) and another 30 mice was injected with Z138 cells (ATM-proficient). Five days following xenograft implantation, mice were injected i.p. daily for 28 consecutive days with either vehicle alone [10% DMSO, 10% (w/v) 2-hydroxy-propyl-β-cyclodextrin in PBS] or 25 or 50 mg/kg olaparib as described previously (36). Tumor volume [0.5 × (width) × (length)^2] was measured manually using a caliper thrice weekly. Mice were sacrificed when tumors reached >1,500 mm^3, weight loss exceeded 20% of initial weight, or at the first obvious signs of distress. Statistical significances of differences in tumor volume were determined using the Student's t test. Kaplan-Meier survival was analyzed by the log-rank (Mantel-Cox) test to determine statistical significance.

Results

Granta-519 and UPN2 Cell Lines Lack Functional ATM

To determine the level of ATM protein expression in the MCL cell lines tested, whole-cell extracts were generated and ATM levels were determined by Western blot. ATM expression in the ATM-proficient lymphoblastoid cell line C35ABR (BT; ref. 37) and the ATM-deficient cell line L3, which was derived from an A-T patient (38), are shown for comparison. ATM protein levels were significantly reduced in whole-cell extracts from Granta-519 and UPN2 compared with BT, HBL-2, JVM-2, UPN1, and Z138 cell lines (Fig. 1A and B). The amount of ATM protein in Granta-519 and UPN2 cells was estimated to be 25% and <5%, respectively, of that in BT cells (Fig. 1B). As expected, ATM protein was undetectable in L3 cells (Fig. 1A and B).

To test for ATM function, we characterized ATM-dependent signaling pathways following DNA damage. IR induces DSBs that lead to activation of the protein kinase activity of ATM and phosphorylation of multiple downstream target proteins, including SMC-1 and KAP-1, which in turn leads to cell cycle checkpoint arrest, DNA repair, or cell death (20, 21). One of the most well-characterized indicators of ATM activity is autophosphorylation on Ser^{1981} (39). We first characterized IR-induced DNA damage signaling in BT (ATM-proficient) and L3 (ATM-deficient) lymphoblastoid cell lines to determine the level of ATM dependency of various phosphorylation events in B cells (Supplementary Fig. S1). As expected, autophosphorylation of ATM on Ser^{1981} occurred rapidly in BT cells and was maintained for at least 2 h but was not detected in the ATM-defective L3 cell line. Similarly, IR-induced phosphorylation of SMC-1 (Ser^{957}) and KAP-1 (Ser^{824}) was highly ATM dependent (Supplementary Fig. S1A and B). The residual IR-induced phosphorylation observed on SMC-1 (Ser^{966}) and KAP-1 (Ser^{824}) in L3 cells (Supplementary Fig. S1B) is likely due to the activity of a related protein kinase such as DNA-PK or ATM- and Rad3-related ATR, which phosphorylate many target proteins in a redundant manner to ATM (40, 41).

ATM-dependent signaling pathways were then examined in the panel of MCL cell lines. Autophosphorylation

Published OnlineFirst February 2, 2010; DOI: 10.1158/1535-7163.MCT-09-0872

of ATM on Ser[1981] was detected in the ATM-positive cell lines HBL-2, JVM-2, UPN1, and Z138 but undetectable in the ATM-deficient cell lines Granta-519 and UPN2 (Fig. 2; Supplementary Fig. S2). The MAVER-1 cell line, in which one *ATM* allele is deleted (26), also underwent Ser[1981] phosphorylation, suggesting that the residual ATM is still active in this cell line (Supplementary Fig. S2B). Phosphorylation of SMC-1 (Ser[957] and Ser[966]) as well as KAP-1 (Ser[824]) was dramatically reduced in both Granta-519 and UPN2 cells compared with HBL-2, JVM-2, MAVER-1, UPN1, and Z138 (Fig. 2; Supplementary Fig. S2). Thus, IR-induced, ATM-dependent signaling pathways appear intact in HBL-2, JVM-2, MAVER-1, UPN1, and Z138 but are defective in Granta-519 and UPN2.

One of the defining features of cells deficient in ATM function is sensitivity to IR (20). To examine the IR sensitivity of the MCL cell lines, cellular viability was determined 96 h following 2 Gy IR using the WST-1 assay (Fig. 1C). Each of the MCL cell lines displayed increased sensitivity to IR compared with the control lymphoblastoid cell line (BT), consistent with previous reports suggesting that MCL cells are radiosensitive (25). However, the ATM-deficient cell lines Granta-519 and UPN2 were significantly more radiosensitive than their ATM-proficient counterparts; indeed, radiosensitivity in these cell lines was comparable with that of the A-T–derived (ATM-deficient) cell line (L3; Fig. 1C).

Another primary ATM function is initiation of cell cycle checkpoint arrest in response to DNA damage. The damage-induced initiation of the G_2-M checkpoint is critical for preventing cells from passing damaged chromosomes to daughter cells, which could result in aneuploidy and oncogenic transformation (42). Initiation of the G_2-M checkpoint was examined using phosphorylation of histone H3 at Ser[10] as a marker of entry into mitosis (35). BT and L3 cells were used as positive and negative controls, respectively. The fraction of cells in mitosis in the ATM-proficient cells (BT, UPN1, and Z138) 1 h post-IR was dramatically reduced, consistent with an intact G_2-M checkpoint (Fig. 1D, gray columns). In contrast, in the ATM-deficient cell lines (L3, Granta-519, and UPN2), a significant proportion of the cells remained in mitosis 1 h post-IR (Fig. 1D, gray columns). In the ATM-deficient cell lines, the percentage of cells entering mitosis was further reduced at 24 h, whereas the fraction of cells in mitosis 24 h post-IR in the ATM-proficient cells was

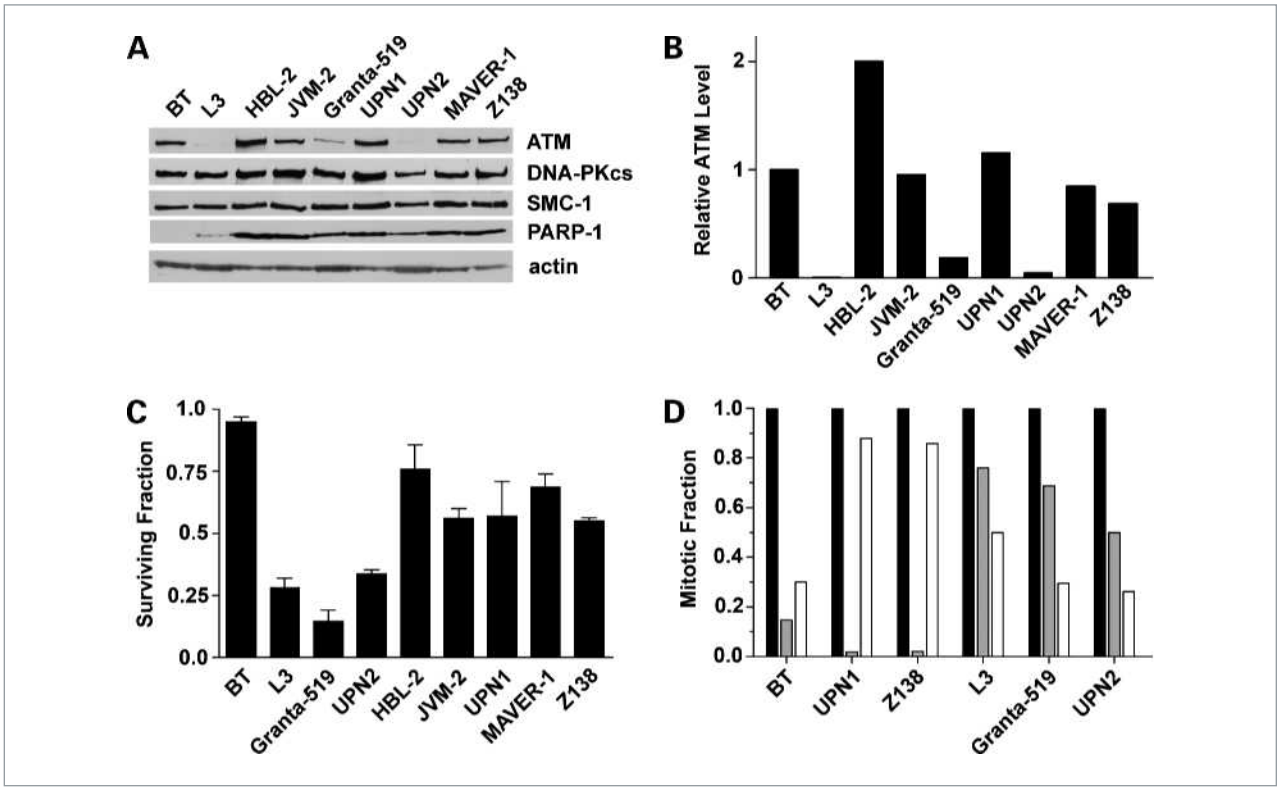

Figure 1. Deficiency of ATM level and function in Granta-519 and UPN2 cell lines. A, relative levels of expression of ATM, DNA-PKcs, SMC-1, and PARP-1 proteins in the MCL cell lines HBL-2, JVM-2, Granta-519, UPN1, UPN2, MAVER-1, and Z138 compared with a control lymphoblastoid cell line C35ABR (BT) and an A-T patient-derived lymphoblastoid cell line (L3). B, ATM protein levels in A were quantitated and normalized to the levels of DNA-PKcs and SMC-1 in BT cells. C, BT, L3, and MCL cell lines were either unirradiated or irradiated with 2 Gy IR, and cellular viability was determined after 96 h using the WST-1 assay. The fraction of viable cells normalized to the untreated control of each cell line is shown. D, cells were either untreated (black columns) or irradiated with 2 Gy IR, collected either 1 h (gray columns) or 24 h (white columns) later, and assayed for phospho-Ser[20] histone H3 phosphorylation as described in Materials and Methods. The percentage of cells in mitosis was normalized to the untreated control of each cell line to give the mitotic fraction.

Published OnlineFirst February 2, 2010; DOI: 10.1158/1535-7163.MCT-09-0872

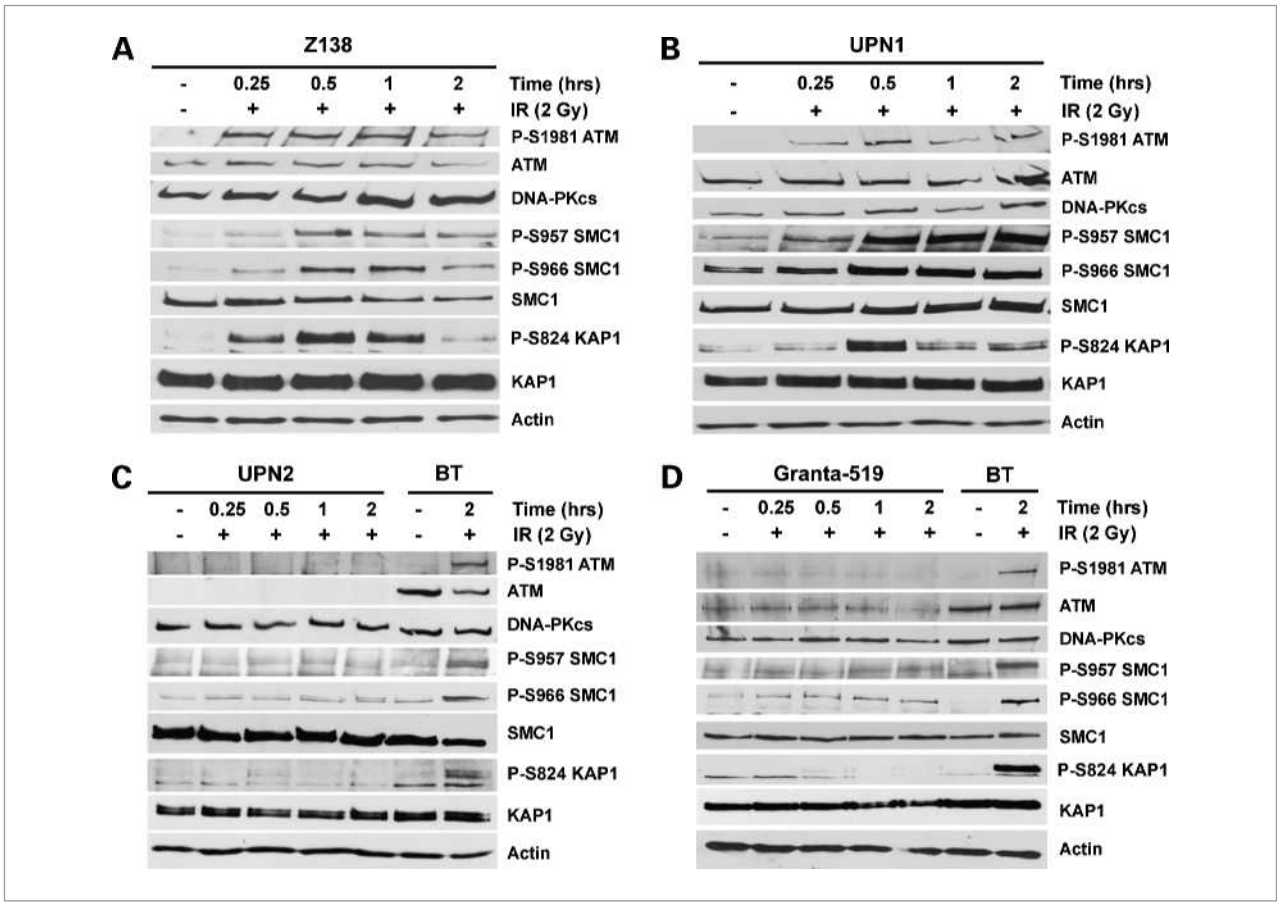

Figure 2. ATM-dependent signaling is reduced in Granta-519 and UPN2 cell lines. MCL cell lines were exposed to 2 Gy IR and harvested following the indicated incubation times. The ATM-proficient lymphoblastoid cell line BT is shown in C and D as a positive control for ATM-dependent signaling. Whole-cell extracts (50 μg total protein) were analyzed by SDS-PAGE and immunoblotted for autophosphorylation of ATM on Ser^{1981} (P-S1981), phosphorylation of SMC-1 on Ser^{957} and Ser^{966} (P-S957 and P-S966, respectively), and phosphorylation of KAP-1 on Ser^{824} (P-S824). Total ATM, SMC-1, and KAP-1 protein levels are also shown. Actin and DNA-PKcs are shown as loading controls. A, Z138; B, UPN1; C, UPN2; D, Granta-519. Signaling pathways in BT, L3, HBL-2, JVM-2, and MAVER-1 cells are shown in Supplementary Figs. S1 and S2.

increased (Fig. 1D, white columns). This result is consistent with the presence of a late-acting, ATR–dependent cell cycle checkpoint in ATM-deficient cells (35). Together, these experiments show that ATM functions normally in HBL-2, JVM-2, MAVER-1, UPN1, and Z138 cells, whereas *ATM* alterations in Granta-519 and UPN2 disrupt ATM function.

ATM-Deficient MCL Cell Lines Are Sensitive to PARP-1 Inhibition

To test whether the ATM-deficient MCL cell lines were sensitive to PARP-1 inhibition, we used PJ34 and olaparib, which inhibit 50% of PARP-1 activity (IC_{50}) *in vitro* at 30 and 5 nmol/L, respectively (29, 30). Cells were incubated with increasing concentrations of either PJ34 (Fig. 3A) or olaparib (Fig. 3B) for 96 h, and viability was assessed by trypan blue exclusion. As expected, the ATM-deficient A-T cell line L3 was more sensitive to PARP-1 inhibition than the ATM-proficient cell line (BT; Fig. 3A and B). Moreover, Granta-519 and UPN2 were also significantly more sensitive to PARP-1 inhibition than were any of the ATM-proficient MCL cell lines tested (HBL-2, JVM-2, UPN1, and Z138; Fig. 3A and B). We note that MAVER-1 cells, in which one ATM allele is deleted (Supplementary Table S1), were not sensitive to either PARP-1 inhibitor (Fig. 3A and B, black triangles). MAVER-1 cells were also shown to have functional ATM signaling pathways (Supplementary Fig. S2B), suggesting that the residual ATM in these cells is sufficient to protect from synthetic lethality to PARP-1 inhibitors. The effects of PARP inhibition on viability of Granta-519, HBL-2, JVM-2, UPN2, and Z128 cells were subsequently confirmed using the WST-1 cytotoxicity assay. Viability of BT, L3, and the MCL cell lines was determined 96 h following treatment with either 10 μmol/L PJ34 (Fig. 3C) or 5 μmol/L olaparib (Fig. 3D). Again, decreased cellular viability was observed in the ATM-deficient cell lines treated with either PJ34 or olaparib. Asterisks represent statistically significant differences between BT and L3 and between Granta-519 and HBL-2, JVM-2, and Z138 (Fig. 3C). With olaparib, statistically significant differences were seen between BT and L3 and

Published OnlineFirst February 2, 2010; DOI: 10.1158/1535-7163.MCT-09-0872

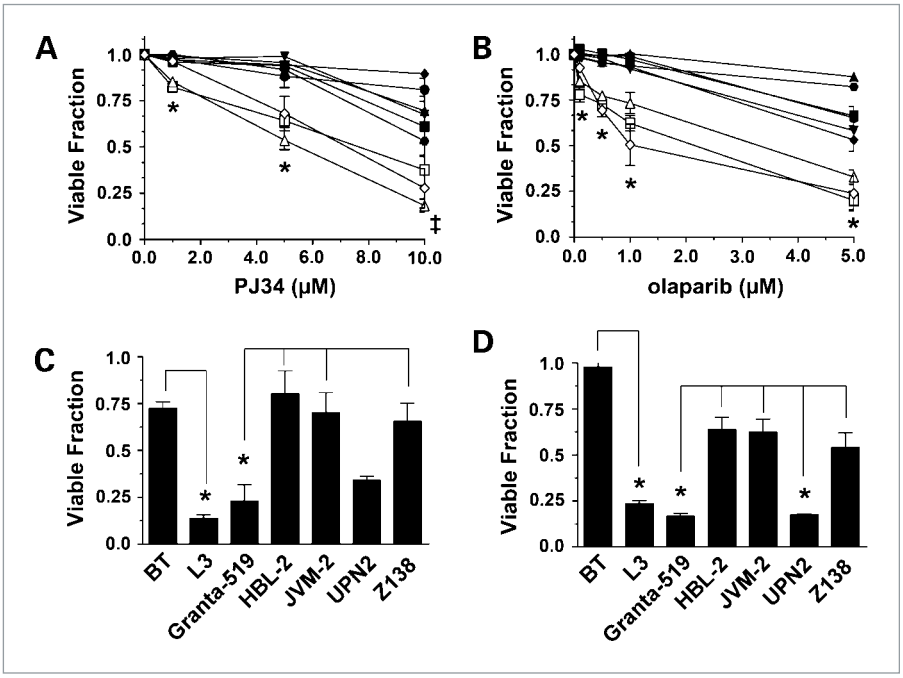

Figure 3. PARP-1 inhibitors preferentially target ATM-deficient MCL cells. BT, L3, and MCL cell lines were exposed to the indicated concentrations of PJ34 (A) or olaparib (B) or vehicle control for 96 h, and cellular viability was determined by trypan blue exclusion. Cell viability was normalized to the vehicle-treated control for each cell line. White triangles, Granta-519; black triangles, HBL-2; inverted black triangles, JVM-2; black diamonds, MAVER-1; black circles, UPN1; white squares, UPN2; black squares, Z138; black hexagons, BT; white diamonds, L3. Bars, SE. *, $P < 0.05$, statistical significance between ATM-proficient and ATM-deficient MCL cell lines. A, ‡, $P < 0.05$, statistically significant difference between Granta-519 and ATM-proficient MCL cell lines. C, BT, L3, and MCL cell lines were incubated with vehicle alone or PJ34 (10 μmol/L) for 96 h after which cell viability was determined using the WST-1 assay. Cell viability was normalized to the vehicle-treated control for each cell line. D, cells were treated with vehicle alone or olaparib (5 μmol/L). After 96 h, cell viability was determined as in C. Bars, SE. C and D, *, $P < 0.05$, statistical significance between BT and L3 and between ATM-proficient and ATM-deficient MCL cell lines. The line indicates which experimental parameters are being compared. In each experiment, BT cells are compared with L3 cells, whereas all MCL cell lines are compared with each other.

between Granta-519 and UPN2 and HBL-2, JVM-2, and Z138 (Fig. 3D).

Because the MCL cell lines analyzed were derived from different patient samples and therefore are not isogenic, we sought additional evidence that the cytotoxicity of PARP-1 inhibitors was indeed due to reduced ATM function. ATM protein was depleted in Z138 cells (ZC-shATM) using a vector expressing a shRNA to ATM that has been shown previously to stably reduce ATM levels in neural cells (32). As a control, Z138 cells were stably transfected with shRNA to GFP (ZC-shGFP). The level of ATM protein in ZC-shATM cells was determined by immunoblot and compared with levels in BT and L3 cells, the parental control Z138, and the knockdown control ZC-shGFP (Fig. 4A). ATM protein levels in ZC-shATM were reduced by at least 75% compared with the levels in either Z138 or ZC-shGFP (Supplementary Fig. S3). Reduction of ATM levels in the knockdown cell line had no effect on the expression of DNA-PKcs, SMC-1, PARP-1, or cyclin D1 (Fig. 4A). As expected, ATM-dependent signaling was reduced in ZC-shATM as indicated by reduced autophosphorylation of ATM following 2 Gy IR (Fig. 4B). We next tested whether the ATM knockdown cells were sensitive to PARP-1 inhibition. For these and subsequent experiments, we focused on olaparib rather than on PJ34, as olaparib is a clinically relevant PARP inhibitor that has antitumor activity toward cancers with mutations in BRCA1 or BRCA2 (36, 43). Importantly, the ATM knockdown cell line ZC-shATM was significantly more sensitive to olaparib when compared with either Z138 or ZC-shGFP cells as determined by either trypan blue exclusion (Fig. 4C) or the WST-1 cytotoxicity assay (Fig. 4D). Together, these results further confirm that loss or reduction of ATM function in MCL cell lines leads to increased sensitivity to PARP-1 inhibition.

Mechanism of PARP Inhibitor-Induced Cell Death in MCL Cell Lines

It has been proposed that inhibition of PARP-1 leads to accumulation of DNA single-strand breaks that are converted to DSBs during DNA replication. In DSB repair-competent cells, these DSBs are repaired, whereas in cells with defects in pathways for DSB detection and/or repair these DSBs induce cell death (2–5). In keeping with this, PARP-1 inhibitors have been shown to induce ATM autophosphorylation on Ser^{1981} as well as phosphorylation of downstream ATM targets, Chk2, Nbs1, and H2AX (9, 11, 36). To determine the mechanism of cell death in olaparib-treated MCL cells, we asked whether olaparib induced phosphorylation of ATM on Ser^{1981}. The

Published OnlineFirst February 2, 2010; DOI: 10.1158/1535-7163.MCT-09-0872

ATM-proficient cell lines Z138 and UPN1 and the ATM-deficient cell lines Granta-519 and UPN2 were exposed to 2.5 μmol/L olaparib for up to 96 h, and ATM autophosphorylation was determined by Western blot. In Z138 (Fig. 5A) and UPN1 (Supplementary Fig. S4) cells, olaparib induced ATM Ser^{1981} autophosphorylation by 24 h, with the relative amount of phosphorylation increasing over time up to 96 h. As expected, no phosphorylation of Ser^{1981} was detected in the ATM-deficient cell lines, Granta-519 (Fig. 5A) or UPN2 (Supplementary Fig. S4). These results are consistent with olaparib inducing DSBs in MCL cells. To determine whether cell death was occurring via apoptosis, cells were analyzed using TUNEL assays and Annexin V staining. ATM-deficient UPN2 and Granta-519 cells displayed a 15- to 20-fold increase in TUNEL-positive (apoptotic) cells compared with untreated cells (Fig. 5B). This contrasts with ATM-proficient UPN1 and Z138 cells, where only a slight increase in apoptotic cells was seen over untreated controls. Moreover, a significant increase in the percentage of Annexin V–positive apoptotic cells was observed in both Granta-519 and UPN2 cells on treatment with olaparib, whereas few apoptotic cells were seen in Z138 or UPN1 cell lines (Fig. 5C). Thus, we conclude that olaparib induces DSBs and that cell death occurs, at least in part, by apoptosis (Fig. 5D).

Olaparib Reduces Tumor Growth and Improves Survival in an *In vivo* Mouse Model for MCL

To test the effectiveness of olaparib in an *in vivo* setting, we used a mouse xenograft model of MCL (31). Immunocompromised RAG2-deficient mice were inoculated s.c. with either Granta-519 or Z138 cells. Beginning 5 days after inoculation, mice were injected i.p. with vehicle alone, 25 or 50 mg/kg olaparib, every day for 28 consecutive days. Notably, a statistically significant reduction in tumor growth was observed in mice bearing Granta-519 xenografts at both 25 and 50 mg/kg (Fig. 6A). Moreover, olaparib significantly prolonged the survival of these mice in a dose-dependent manner (Fig. 6B). The median survival of the control group (28 days) was extended by 25% (to 35 days) for mice receiving 25 mg/kg and 42% (to 40 days) for mice receiving 50 mg/kg olaparib. In contrast, in mice bearing Z138 xenografts, the difference in tumor growth rate between control mice and mice receiving 25 mg/kg olaparib was not statistically significant, and only a modest lag in tumor growth was

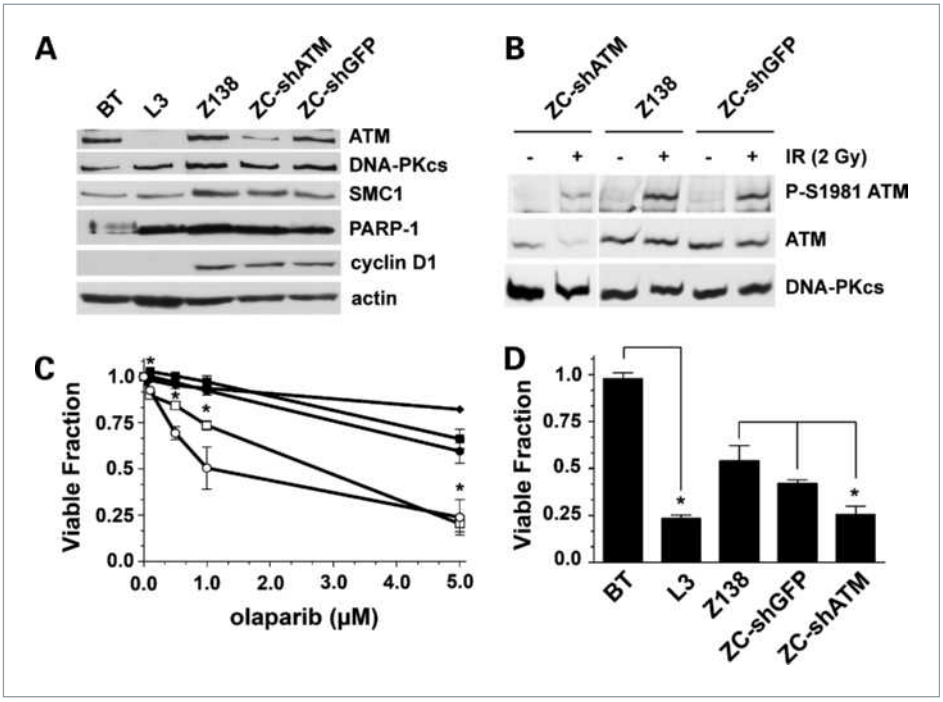

Figure 4. Inhibition of PARP-1 is cytotoxic in MCL cells with reduced ATM protein expression. A, Z138 cells were stably transfected with a vector expressing shRNA targeting ATM (ZC-shATM) or GFP (ZC-shGFP) as a negative control as described in Materials and Methods. Whole-cell extracts (50 μg) were run on SDS-PAGE, and immunoblots were probed for ATM, DNA-PKcs, SMC-1, PARP-1, cyclin D1, and actin protein expression. B, Z138, ZC-shGFP, or ZC-shATM cells were either unirradiated (–) or irradiated (2 Gy) and harvested following a 2 h incubation. Whole-cell extracts were probed for phosphorylated ATM (P-S1981), total ATM, and DNA-PKcs. C, cells were incubated with various concentrations of olaparib, and after 96 h, cell viability was determined by trypan blue exclusion. Black squares, Z138; black circles, ZC-shGFP; white squares, ZC-shATM; black diamonds, BT; white circles, L3. *, $P < 0.05$, statistical significance between ZC-shATM and Z138/ZC-shGFP. D, BT, L3, Z138, ZC-shGFP, and ZC-shATM cells were exposed to olaparib (5 μmol/L) for 96 h and cellular viability was determined using the WST-1 assay. Bars, SE. In each experiment, BT cells are compared with L3 cells, whereas all MCL cell lines are compared with each other.

Published OnlineFirst February 2, 2010; DOI: 10.1158/1535-7163.MCT-09-0872

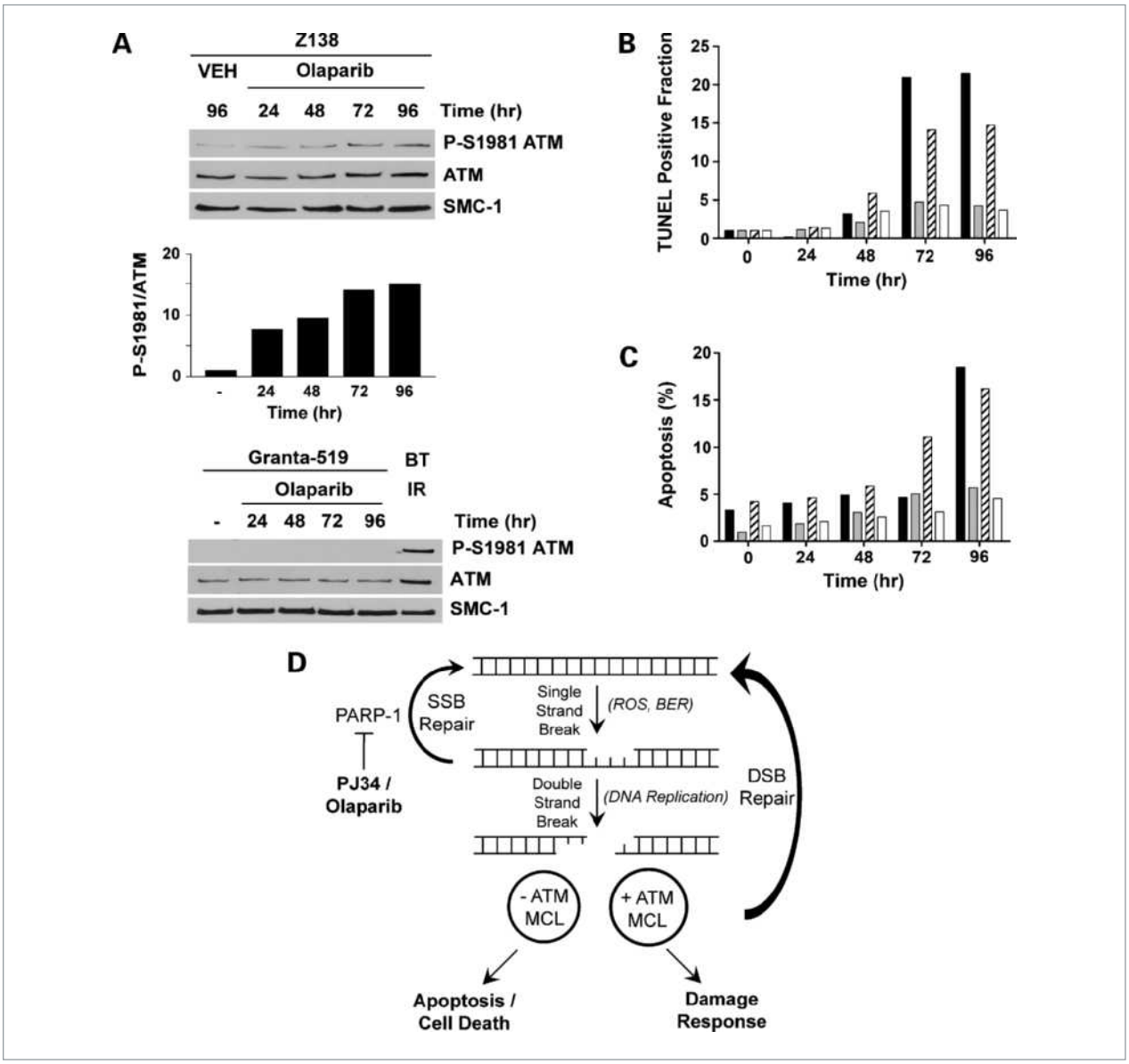

Figure 5. Olaparib induces Ser[1981] phosphorylation in ATM-proficient MCL cells and apoptosis in ATM-deficient MCL cells. A, Z138 and Granta-519 cells were exposed to olaparib (2.5 μmol/L) or vehicle (VEH; DMSO) for 24, 48, 72, or 96 h. Whole-cell extracts (50 μg total protein) were run on SDS-PAGE, immunoblotted, and probed for ATM autophosphorylation at Ser[1981] (P-S1981), total ATM, and total SMC-1. Quantitation of olaparib-induced P-S1981 ATM compared with total ATM for Z138 is shown below the blot. As a positive control for P-Ser[1981], in the Granta-519 cells, BT cells were irradiated 2 Gy and harvested after 1 h. B, cells were treated with 2.5 μmol/L olaparib for 24, 48, 72, or 96 h, and the proportion of cells undergoing apoptosis was determined using the TUNEL assay. The fraction of TUNEL-positive cells was normalized to the untreated sample for each cell line. Results are presented as the percentage of TUNEL-positive cells at each time point. Black columns, Granta-519; gray columns, UPN1; hatched columns, UPN2; white columns, Z138. C, cells were treated with olaparib and assayed for Annexin V and propidium iodide staining. The percentage of apoptotic cells (+ for Annexin V and – for propidium iodide) is shown. Column shading is as in B. D, a model for the mechanism of PARP-1–induced cell death. DNA single-strand breaks generated in cells by reactive oxygen species (ROS) or as intermediates during base excision repair (BER) are recognized by PARP-1 and repaired by the base excision and/or DNA single-strand break repair pathways. Small-molecule inhibitors of PARP-1 (e.g., PJ34 or olaparib) block single-strand break repair, permitting the conversion of single-strand breaks into DNA DSBs during DNA replication. MCL cells with wild-type ATM initiate an appropriate DSB damage response and survive, whereas cells in which ATM function is disrupted have reduced ability to respond to DNA DSBs, resulting in cell death via apoptosis.

observed at higher doses of olaparib (50 mg/kg; Fig. 6C). The effect of olaparib on the Z138 xenografts at high doses of olaparib was not unexpected, as high doses also decreased viability of Z138 cells in *in vitro* cytotoxicity assays (Fig. 3). Median survival of the Z138 control group (44 days) was the same as the group receiving 25 mg/kg olaparib (44 days) and increased by 23% (54 days) for mice receiving 50 mg/kg (Fig. 6D).

Published OnlineFirst February 2, 2010; DOI: 10.1158/1535-7163.MCT-09-0872

Discussion

The synthetic lethal approach using PARP inhibitors represents a powerful new strategy for therapeutic intervention (2–5). To date, this approach has been validated for breast and ovarian cancers (43); however, whether it is applicable to other human cancers is not known. Here, we addressed this question for MCL, an aggressive B-cell lymphoma, which represents ~10% of all cases of non-Hodgkin's lymphoma.

Characterization of ATM function in a panel of seven MCL cell lines showed reduced ATM function in Granta-519 and UPN2 cells. Consistent with previous results, no ATM protein was detected in UPN2 (25). Although Granta-519 contained low levels of ATM protein, no Ser^{1981} phosphorylation was detected and the cells were highly radiation sensitive and exhibited cell cycle checkpoint defects, consistent with lack of functional ATM. Previously reported alterations of *ATM* in UPN1 (25) and MAVER-1 (26) appeared to have little effect on ATM function, as ATM-dependent signaling, checkpoint arrest, and sensitivity to IR were all similar to that observed in control lymphoblastoid cells and the other ATM-proficient MCL cell lines.

Significantly, Granta-519 and UPN2 cell lines were significantly more sensitive to PARP-1 inhibitors than were the ATM-proficient MCL cell lines examined. The LD_{50} using the clinically relevant PARP-1 inhibitor olaparib was 3.3 μmol/L for Granta-519 and 2.1 μmol/L for UPN2 (Fig. 3B). The toxicity of PARP-1 inhibition was further confirmed in MCL cells in which ATM protein levels were stably reduced by shRNA. The LD_{50} for olaparib in the ATM knockdown cell line ZC-shATM was 2.7 μmol/L, which was comparable with the values obtained in other ATM-deficient MCL cell lines and was significantly lower

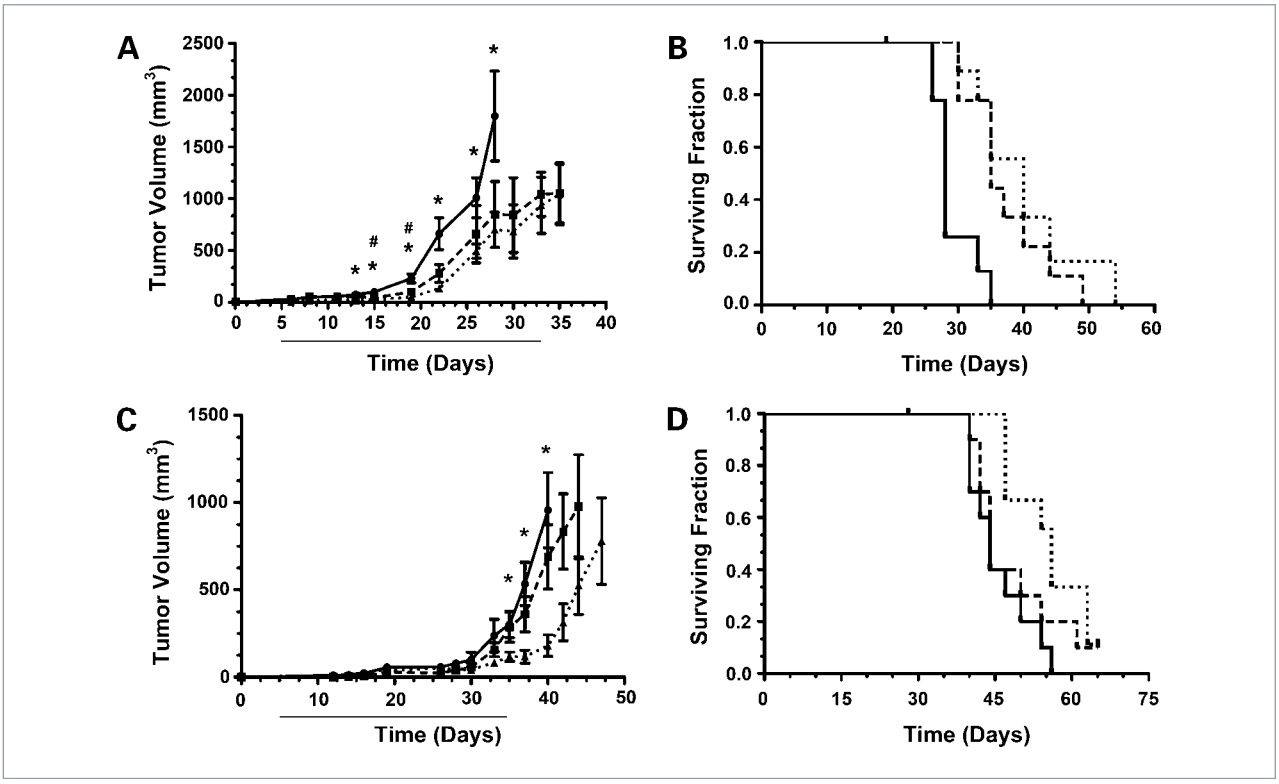

Figure 6. Olaparib reduces tumor growth and prolongs survival of mice bearing ATM-deficient xenografts. A, mice were injected s.c. with Granta-519 (ATM-deficient) cells as described in Materials and Methods. Five days later, mice were injected i.p. with vehicle alone (circles, solid lines), 25 mg/kg olaparib (squares, dashed lines), or 50 mg/kg olaparib (triangles, dotted lines). Injections of drug/vehicle were continued for 28 consecutive days (solid line beneath the *X* axis). Tumor volume was determined as described in Materials and Methods. $n = 8$ mice for the 0 and 50 mg/kg groups and $n = 9$ for the 25 mg/kg group. Bars, SE. * and #, $P > 0.05$, statistical significance as determined by the Student's *t* test between control and olaparib-treated mice (50 and 25 mg/kg groups, respectively). B, survival curves for the experiment shown in A. Solid lines, mice injected with vehicle alone; dashed and dotted lines, mice treated with 25 or 50 mg/kg olaparib, respectively. Endpoint survival at 25 and 50 mg/kg was considered statistically significant ($P = 0.0018$ and 0.0012, respectively) compared with vehicle-treated animals using the Mantel-Cox test. Mean survival times were 28 days (vehicle alone), 35 days (25 mg/kg olaparib), and 40 days for 50 mg/kg olaparib. C, tumor volume for mice injected with Z138 cells (ATM-proficient) followed by injection with vehicle alone (circles, solid lines), 25 mg/kg olaparib (squares, dashed lines), or 50 mg/kg olaparib (triangles, dotted lines) as described in A. $n = 10$ mice for the 0 and 25 mg/kg groups and $n = 9$ for the 50 mg/kg group. Bars, SE. *, $P > 0.05$, statistically significant as determined by the Student's *t* test (50 mg/kg group compared with vehicle-treated controls). D, survival curves for the experiment shown in C. Solid lines, vehicle alone; dashed lines, 25 mg/kg olaparib; dotted lines, 50 mg/kg olaparib. Endpoint survival between 0 and 25 mg/kg was not considered statistically significant ($P = 0.316$). Endpoint survival between and 0 and 50 mg/kg was considered statistically significant ($P = 0.0057$) using the Mantel-Cox test. Mean survival of mice receiving no olaparib was 45 days compared with 45 and 56 days for mice receiving 25 or 50 mg/kg olaparib, respectively.

Published OnlineFirst February 2, 2010; DOI: 10.1158/1535-7163.MCT-09-0872

than the LD_{50} for olaparib in either the control knockdown or parental control cell lines (>5 μmol/L; Fig. 4C).

Autophosphorylation of ATM on Ser^{1981} in the ATM-proficient MCL cell lines following olaparib treatment indicates that inhibition of PARP-1 leads to the induction of DNA DSBs and activation of an ATM-dependent DNA damage response pathway. We propose that ATM-proficient MCL cells retain the ability to respond to such damage, whereas impairment of ATM function in Granta-519 and UPN2 cells should lead to persistent unrepaired DSBs resulting in increased cell death (Fig. 5D). Our results further suggest that apoptosis plays a role in PARP-1 inhibitor-induced cell death in ATM-deficient MCL cells. Indeed, apoptosis occurs in BRCA1- or BRCA2-deficient cells treated with PARP-1 inhibitors (7, 36).

ATM and p53 status are proposed to be critical in determining the cellular response to chemotherapy (44); however, the p53 status of the MCL cell lines examined here does not appear to correlate with sensitivity to PARP-1 inhibitors. For example, Granta-519 cells have one wild-type p53 allele, whereas p53 is mutant in UPN2 (Supplementary Table S1), yet both are sensitive to PARP-1 inhibitors. Also, of the MCL cell lines that were resistant to PARP-1 inhibition, some are reported to contain mutations or deletions in *p53* (MAVER-1, UPN1, and HBL-2), whereas, in others, both alleles of *p53* are wild-type (JVM-2 and Z138; Supplementary Table S1; ref. 28). In addition, p53 status was consistent among ATM knockdown cells (ZC-shATM), control knockdown cells (ZC-shGFP), and parental cells (Z138; Fig. 4A); however, ZC-shATM was more sensitive to olaparib than either parental or control cell line. Although the relationship between p53 status and olaparib warrants further study, our results suggest that wild-type p53 is not required for olaparib sensitivity.

To further test the potential of olaparib as a therapeutic agent for MCL, we used an *in vivo* xenograft model using both ATM-deficient (Granta-519) and ATM-proficient (Z138) cells (Fig. 6). Significantly, PARP-1 inhibition by olaparib reduced tumor growth and increased survival in a dose-dependent manner in mice bearing xenografts of ATM-deficient cells (Fig. 6A and B). Although olaparib also reduced tumor growth and increased survival in xenografts with ATM-proficient tumors, this effect was only seen at the higher dose (50 mg/kg; Fig. 6C and D).

Our results suggest that PARP-1 inhibitors have potential in the treatment of malignancies in which the response to and/or repair of DNA damage is compromised and that the concept of synthetic lethality, initially developed for breast and ovarian cancers characterized by mutations in *BRCA1* or *BRCA2* (45), can also be extended to MCL cells with alterations in *ATM*. Moreover, as most *ATM* alterations seen in MCL occur only in malignant B cells not in other somatic tissues (18, 46), the use of PARP-1 inhibitors in MCL has the potential to offer a targeted approach to cancer therapy. We also note that the synthetic lethal approach may be applicable to other tumors with alterations in ATM, including B-cell chronic lymphocytic leukemia (19, 47) and non–small cell lung cancer (48, 49) as well as gastric cancer (50). Thus, targeting ATM-defective tumors by PARP-1 inhibitors may have broad utility beyond MCL.

Disclosure of Potential Conflicts of Interest

M.J. O'Connor is an employee of KuDOS Pharmaceuticals, a wholly owned subsidiary of AstraZeneca.

Acknowledgments

We thank Dr. Y. Shiloh (Tel Aviv University) for shRNA vectors to ATM and GFP; Drs. Y. Shiloh and M. Lavin (Queensland Institute for Medical Research) for cell lines; L. Robertson, L. Kennedy, and the University of Calgary Flow Cytometry Facility for assistance with the fluorescence-activated cell sorting experiments; M. Chisholm and the University of Calgary Animal Resource Centre; Dr. A. Cranston (KuDOS Pharmaceuticals) for advice on *in vivo* experiments; Dr. D. Proud and laboratory members for use of the ELISA plate reader; Drs. S. Robbins and E. Kurz and the members of the S.P. Lees-Miller laboratory for discussions; and Dr. J. Tainer for helpful comments on the article.

Grant Support

National Cancer Institute of Canada grant 016253 with funds from the Canadian Cancer Society and National Institutes of Health P01 grant CA92584 (S.P. Lees-Miller) and a grant from the Leukemia and Lymphoma Society of Canada (D.G. Bebb and S.P. Lees-Miller). C.T. Williamson was supported by graduate studentships from Alberta Health Services and Translational Research in Cancer Program with funds from the Canadian Institutes of Health Research and the Alberta Cancer Foundation. H.M was partially supported by Alberta Health Services grant 22470. S.P. Lees-Miller holds the Engineered Air Chair in Cancer Research and is a Scientist of the Alberta Heritage Foundation for Medical Research.

The costs of publication of this article were defrayed in part by the payment of page charges. This article must therefore be hereby marked *advertisement* in accordance with 18 U.S.C. Section 1734 solely to indicate this fact.

Received 6/3/09; revised 11/5/09; accepted 11/24/09; published OnlineFirst 2/2/10.

References

1. Hoeijmakers JH. Genome maintenance mechanisms for preventing cancer. Nature 2001;411:366–74.
2. O'Connor MJ, Martin NM, Smith GC. Targeted cancer therapies based on the inhibition of DNA strand break repair. Oncogene 2007;26:7816–24.
3. Martin SA, Lord CJ, Ashworth A. DNA repair deficiency as a therapeutic target in cancer. Curr Opin Genet Dev 2008;18:80–6.
4. Lord CJ, Ashworth A. Targeted therapy for cancer using PARP inhibitors. Curr Opin Pharmacol 2008;8:363–9.
5. Helleday T, Petermann E, Lundin C, Hodgson B, Sharma RA. DNA repair pathways as targets for cancer therapy. Nat Rev Cancer 2008;8:193–204.
6. Schreiber V, Dantzer F, Ame JC, de Murcia G. Poly(ADP-ribose): novel functions for an old molecule. Nat Rev Mol Cell Biol 2006;7:517–28.
7. Farmer H, McCabe N, Lord CJ, et al. Targeting the DNA repair defect in BRCA mutant cells as a therapeutic strategy. Nature 2005;434:917–21.

Published OnlineFirst February 2, 2010; DOI: 10.1158/1535-7163.MCT-09-0872

8. Bryant HE, Schultz N, Thomas HD, et al. Specific killing of BRCA2-deficient tumours with inhibitors of poly(ADP-ribose) polymerase. Nature 2005;434:913–7.
9. McCabe N, Turner NC, Lord CJ, et al. Deficiency in the repair of DNA damage by homologous recombination and sensitivity to poly(ADP-ribose) polymerase inhibition. Cancer Res 2006;66:8109–15.
10. Lord CJ, McDonald S, Swift S, Turner NC, Ashworth A. A high-throughput RNA interference screen for DNA repair determinants of PARP inhibitor sensitivity. DNA Repair (Amst) 2008;7:2010–9.
11. Bryant HE, Helleday T. Inhibition of poly (ADP-ribose) polymerase activates ATM which is required for subsequent homologous recombination repair. Nucleic Acids Res 2006;34:1685–91.
12. Gaymes TJ, Shall S, Farzaneh F, Mufti GJ. Chromosomal instability syndromes are sensitive to poly ADP-ribose polymerase inhibitors. Haematologica 2008;93:1886–9.
13. Haince JF, Kozlov S, Dawson VL, et al. Ataxia telangiectasia mutated (ATM) signaling network is modulated by a novel poly(ADP-ribose)-dependent pathway in the early response to DNA-damaging agents. J Biol Chem 2007;282:16441–53.
14. Bertoni F, Rinaldi A, Zucca E, Cavalli F. Update on the molecular biology of mantle cell lymphoma. Hematol Oncol 2006;24:22–7.
15. Jares P, Colomer D, Campo E. Genetic and molecular pathogenesis of mantle cell lymphoma: perspectives for new targeted therapeutics. Nat Rev Cancer 2007;7:750–62.
16. Resnitzky D, Gossen M, Bujard H, Reed SI. Acceleration of the G_1-S phase transition by expression of cyclins D1 and E with an inducible system. Mol Cell Biol 1994;14:1669–79.
17. Kienle D, Katzenberger T, Ott G, et al. Quantitative gene expression deregulation in mantle-cell lymphoma: correlation with clinical and biologic factors. J Clin Oncol 2007;25:2770–7.
18. Schaffner C, Idler I, Stilgenbauer S, Dohner H, Lichter P. Mantle cell lymphoma is characterized by inactivation of the ATM gene. Proc Natl Acad Sci U S A 2000;97:2773–8.
19. Fang NY, Greiner TC, Weisenburger DD, et al. Oligonucleotide microarrays demonstrate the highest frequency of ATM mutations in the mantle cell subtype of lymphoma. Proc Natl Acad Sci U S A 2003;100:5372–7.
20. Shiloh Y. The ATM-mediated DNA-damage response: taking shape. Trends Biochem Sci 2006;31:402–10.
21. Lavin MF. Ataxia-telangiectasia: from a rare disorder to a paradigm for cell signalling and cancer. Nat Rev Mol Cell Biol 2008;9:759–69.
22. Aguilar-Quesada R, Munoz-Gamez JA, Martin-Oliva D, et al. Interaction between ATM and PARP-1 in response to DNA damage and sensitization of ATM deficient cells through PARP inhibition. BMC Mol Biol 2007;8:29.
23. Ferrer A, Marce S, Bellosillo B, et al. Activation of mitochondrial apoptotic pathway in mantle cell lymphoma: high sensitivity to mitoxantrone in cases with functional DNA-damage response genes. Oncogene 2004;23:8941–9.
24. Vorechovsky I, Luo L, Dyer MJ, et al. Clustering of missense mutations in the ataxia-telangiectasia gene in a sporadic T-cell leukaemia. Nat Genet 1997;17:96–9.
25. M'Kacher R, Bennaceur A, Farace F, et al. Multiple molecular mechanisms contribute to radiation sensitivity in mantle cell lymphoma. Oncogene 2003;22:7905–12.
26. Zamo A, Ott G, Katzenberger T, et al. Establishment of the MAVER-1 cell line, a model for leukemic and aggressive mantle cell lymphoma. Haematologica 2006;91:40–7.
27. Salaverria I, Perez-Galan P, Colomer D, Campo E. Mantle cell lymphoma: from pathology and molecular pathogenesis to new therapeutic perspectives. Haematologica 2006;91:11–6.
28. Bea S, Salaverria I, Armengol L, et al. Uniparental disomies, homozygous deletions, amplifications, and target genes in mantle cell lymphoma revealed by integrative high-resolution whole-genome profiling. Blood 2009;113:3059–69.
29. Abdelkarim GE, Gertz K, Harms C, et al. Protective effects of PJ34, a novel, potent inhibitor of poly(ADP-ribose) polymerase (PARP) in *in vitro* and *in vivo* models of stroke. Int J Mol Med 2001;7:255–60.
30. Menear KA, Adcock C, Boulter R, et al. 4-[3-(4-Cyclopropanecarbonylpiperazine-1-carbonyl)-4-fluorobenzyl]-2H-phth alazin-1-one: a novel bioavailable inhibitor of poly(ADP-ribose) polymerase-1. J Med Chem 2008;51:6581–91.
31. Tucker CA, Bebb G, Klasa RJ, et al. Four human t(11;14)(q13;q32)-containing cell lines having classic and variant features of mantle cell lymphoma. Leuk Res 2006;30:449–57.
32. Elkon R, Rashi-Elkeles S, Lerenthal Y, et al. Dissection of a DNA-damage-induced transcriptional network using a combination of microarrays, RNA interference and computational promoter analysis. Genome Biol 2005;6:R43.
33. Douglas P, Sapkota GP, Morrice N, et al. Identification of *in vitro* and *in vivo* phosphorylation sites in the catalytic subunit of the DNA-dependent protein kinase. Biochem J 2002;368:243–51.
34. Goodarzi AA, Noon AT, Deckbar D, et al. ATM signaling facilitates repair of DNA double-strand breaks associated with heterochromatin. Mol Cell 2008;31:167–77.
35. Xu B, Kim ST, Lim DS, Kastan MB. Two molecularly distinct G(2)/M checkpoints are induced by ionizing irradiation. Mol Cell Biol 2002;22:1049–59.
36. Rottenberg S, Jaspers JE, Kersbergen A, et al. High sensitivity of BRCA1-deficient mammary tumors to the PARP inhibitor AZD2281 alone and in combination with platinum drugs. Proc Natl Acad Sci U S A 2008;105:17079–84.
37. Gueven N, Keating KE, Chen P, et al. Epidermal growth factor sensitizes cells to ionizing radiation by down-regulating protein mutated in ataxia-telangiectasia. J Biol Chem 2001;276:8884–91.
38. Kozlov S, Gueven N, Keating K, Ramsay J, Lavin MF. ATP activates ATM *in vitro*: importance of autophosphorylation. J Biol Chem 2003;278:9309–17.
39. Bakkenist CJ, Kastan MB. DNA damage activates ATM through intermolecular autophosphorylation and dimer dissociation. Nature 2003;421:499–506.
40. Stiff T, O'Driscoll M, Rief N, Iwabuchi K, Lobrich M, Jeggo PA. ATM and DNA-PK function redundantly to phosphorylate H2AX after exposure to ionizing radiation. Cancer Res 2004;64:2390–6.
41. Callen E, Jankovic M, Wong N, et al. Essential role for DNA-PKcs in DNA double-strand break repair and apoptosis in ATM-deficient lymphocytes. Mol Cell 2009;34:285–97.
42. Krempler A, Deckbar D, Jeggo PA, Lobrich M. An imperfect G_2M checkpoint contributes to chromosome instability following irradiation of S and G_2 phase cells. Cell Cycle 2007;6:1682–6.
43. Fong PC, Boss DS, Yap TA, et al. Inhibition of poly(ADP-ribose) polymerase in tumors from BRCA mutation carriers. N Engl J Med 2009;361:123–34.
44. Jiang H, Reinhardt HC, Bartkova J, et al. The combined status of ATM and p53 link tumor development with therapeutic response. Genes Dev 2009;23:1895–909.
45. Ashworth A. A synthetic lethal therapeutic approach: poly(ADP) ribose polymerase inhibitors for the treatment of cancers deficient in DNA double-strand break repair. J Clin Oncol 2008;26:3785–90.
46. Camacho E, Hernandez L, Hernandez S, et al. ATM gene inactivation in mantle cell lymphoma mainly occurs by truncating mutations and missense mutations involving the phosphatidylinositol-3 kinase domain and is associated with increasing numbers of chromosomal imbalances. Blood 2002;99:238–44.
47. Austen B, Powell JE, Alvi A, et al. Mutations in the ATM gene lead to impaired overall and treatment-free survival that is independent of IGVH mutation status in patients with B-CLL. Blood 2005;106:3175–82.
48. Safar AM, Spencer H, Su X, Cooney CA, Shwaiki A, Fan CY. Promoter hypermethylation for molecular nodal staging in non-small cell lung cancer. Arch Pathol Lab Med 2007;131:936–41.
49. Ding L, Getz G, Wheeler DA, et al. Somatic mutations affect key pathways in lung adenocarcinoma. Nature 2008;455:1069–75.
50. Kang B, Guo RF, Tan XH, Zhao M, Tang ZB, Lu YY. Expression status of ataxia-telangiectasia-mutated gene correlated with prognosis in advanced gastric cancer. Mutat Res 2008;638:17–25.

Published OnlineFirst February 2, 2010; DOI: 10.1158/1535-7163.MCT-09-0872

Molecular Cancer Therapeutics

ATM Deficiency Sensitizes Mantle Cell Lymphoma Cells to Poly(ADP-Ribose) Polymerase-1 Inhibitors

Chris T. Williamson, Huong Muzik, Ali G. Turhan, et al.

Mol Cancer Ther 2010;9:347-357. Published OnlineFirst February 2, 2010.